An Efficient CRISPR-Cas9 DNA Editing Methodology Applicable for iPSC Disease Modelling

Atefeh Namipashaki[1], XiaodongLiu[2], Kealan Pugsley[1], Sue Mei Lim[2], Guizhi Sun[2], Marco J. Herold [3,4], Jose M. Polo[2,5], Mark A. Bellgrove [1] and Ziarih Hawi [1*]

1. Turner Institute for Brain and Mental Health, School of Psychological Sciences, Monash University, VIC, Australia
2. Department of Anatomy & Developmental Biology, Development and Stem Cells Program, Monash Biomedicine Discovery Institute, and Australian Regenerative Medicine Institute, Monash University, VIC, Australia.
3. Walter and Eliza Hall Institute of Medical Research, Melbourne, VIC, Australia.
4. Department of Medical Biology, University of Melbourne, Melbourne, VIC, Australia
5. Adelaide Centre for Epigenetics and the South Australian Immunogenomics Cancer Institute, The University of Adelaide, SA, Australia

Author for correspondence

Dr Ziarih Hawi
Turner Institute for Brain and Mental Health
School of Psychological Sciences,
Monash University,
Clayton Campus,
VIC, 3800
Australia.
e-mail: ziarih.hawi@monash.edu

ABSTRACT

The capability to generate induced pluripotent cell (iPSC) lines, in combination with the CRISPR-Cas9 DNA editing technology, offers great promise to understand the underlying genetic mechanisms of human disease. However, technical impediments including, but not limited to, low transfection efficiency, single-cell survival, and high clonal heterogeneity, limit the potential of these techniques. Here we provide an efficient methodology addressing these challenges, resulting in high transfection efficiency exceeding 97% with an increased single cell clone survival rate (up to 70%). These enhancements were accompanied by a high editing efficiency in the range of 48.6 to 57.5%, comparable to existing methods.

Introduction

Despite advances in our ability to detect DNA variants conferring risk to complex genetic conditions, our knowledge of the functional effects of these variants is lagging [1]. Commonly used methods, such as animal models and cancerous cell lines, cannot always resemble disease-relevant genotypic and phenotypic properties [2]. Further, inaccessibility of certain living human tissue (e.g., brain) necessitates the development of relevant experimental models that can elucidate the causal molecular and physiological mechanisms of disease [3]. Induced pluripotent stem cells (iPSCs) provide a valuable alternative to existing methods. Typically derived from skin or blood cells, iPSCs can be reprogrammed into an embryonic-like state and once differentiated, represent an unlimited source of any human tissue type. When derived from patients, iPSCs are genetically enriched for the presenting disease or disorder, recapitulating the complex genetic nature and aetiology of the condition [4]. However, without large samples, comparing iPSCs from patients and controls is often impractical, as interindividual heterogeneity hinders mapping of detectable phenotypic differences to disease status [4]. The combined use if iPSCs and CRISPR-Cas9 DNA editing technology can assist to reduce this heterogeneity by generating isogenic cell lines that share the same genetic background and differ only in a genetic variant of interest (e.g., disease-associated variant or gene). This approach will assist to overcome existing logistical challenges associated with studying the genetics of human health and facilitate functional interrogation of disease relevant gene variants [5]. However, CRISPR-mediated genomic manipulation has been hindered by technical impediments, particularly when using iPSCs. Although significant progress has been made to address these issues, several major problems hampering the application of CRISPR–Cas9 in iPSCs remain unsolved. These include:

1. iPSCs as a primary cell type are difficult to transfect, impairing the delivery of the foreign editing complex [6].
2. High-fidelity DNA damage repair and high rates of iPS cell death following transfection reduces editing efficiency. The latter is due, in part, to the toxicity of the CRISPR-Cas9 complex to the iPSCs, which can activate p53-mediated apoptosis [7].
3. iPSCs are susceptible to dissociation-induced apoptosis [8], making single-cell survival a difficult challenge. As a result, transfected cells are commonly cultured in mixed populations. However, homogeneity/monoclonality is essential to retain the desired genotype, and to facilitate downstream phenotypic characterization.

4. Similarities between the guide RNA(gRNA) and the genomic sequence can lead to unintended off-target DNA editing, complicating the ability to identify the effect of the expected edits in the region of interest [9].

Addressing these challenges is critical, particularly given the demand for efficient variant characterisation methods for the myriad of genomic diseases. In this article, we describe the development of a novel methodology to increase transfection efficiency, cell viability, monoclonality of manipulated cells, and editing efficiency. A schematic representation of our iPSC CRISPR-Cas9 editing methodology is presented in Fig. 1.

Results and discussion

Practical application of our method in three different cell lines (HDFn, HDFa and MICCNi002-A) achieved close to 100% transfection efficiency with up to 70% single-cell clone survival post transfection (Fig. 2a and Supplementary Fig. S1). Importantly, editing was observed across 48.6 to 57.5% of surviving clones, successfully disrupting two independent target loci (intron 6-7 of *HPRT* and exon 1 of the *FOXP2* genes) across the genome (Fig. 2b and Supplementary Table S1).

Transfection of iPSCs. Toxicity associated with CRISPR delivery systems represents a significant barrier to achieving high transfection efficiency. Application of electroporation, although common, is an invasive method, necessitate both electrical shock and cell singularisation. These result in low post-treatment recovery of electroporated cells and increased risk of apoptosis [10]. In contrast, lipofection only requires cells to be dissociated into small clumps (3-10 cells), improving cell survival. Further, stem cell specific reagents, such as the Lipofectamine Stem Transfect Reagent (Invitrogen), effectively induce CRISPR uptake [11,12]. Vector selection also influences transfection success, with protein-based delivery systems such as ribonucleoproteins (RNPs) affording a less toxic alternative to DNA based vectors [13,14]. These protein complexes offer additional benefits to the CRISPR editing process, as their non-integrative mode of action and rapid degradation reduces recutting of the target locus, thereby improving editing efficiency [13,14]. The combined application of Lipofectamine Stem Transfect Reagent and RNP complexes in the current method resulted in a transfection efficiency exceeding 97%, as verified by fluorescence-activated cell sorting (FACS) (Fig. 2a). This represents a substantial improvement to previously reported efficiencies (30-59%) using electroporation and DNA vector-based systems [15-17].

Culturing of FACS-sorted positively transfected iPS cells. Single-cell isolation of transfected cells is essential to establish genetically homogeneous iPSC clones. However, culturing of post-transfection single iPSCs is difficult due to the increased risk of dissociation-induced apoptosis [8]. Although the application of feeder cell layers in culture improves single-cell survival, it cannot guarantee the correct phenotyping, as this method is not xenogeneic-free and potentially influence cell morphology and function beyond genetic variability [16,18]. As such, feeder-free approaches are desirable to facilitate correct phenotyping of disease modelling.

Here, we provide a unique protocol to overcome this issue. Successfully transfected cells were isolated through FACS as single iPSCs in individual wells of a 96-well plate pre-coated with Cell Adhere Laminin-521 (STEMCELL Technologies) containing StemFlex medium (Gibco) and supplemented with CloneR (STEMCELL Technologies). Collectively, these reagents aid single-cell survival through establishment of supportive protein scaffold prior to plating and enhance clonal expansion. Through provision of such an enriched environment, we successfully achieved a high post transfection single-cell clone survival rate ranging between 61.8 to 70.1% which is higher than previously reported (40%) [16]. A schematic figure of our single-cell cloning method compared to other isolation approaches is presented in Supplementary Fig. S1.

Relative to other cell isolation and culturing methods, our approach significantly improves the utility of edited iPSCs for disease modelling. For example, although antibiotic selection methods can identify successfully transfected cells, they cannot isolate single-cell clones, and are therefore inappropriate for establishing homogeneous colonies of the same progeny [15,19]. This issue persists with enrichment methods which typically rely on successive rounds of screening (e.g., using ddPCR, T7EN1 assay, and Surveyor assay) and sorting to increase the percentage of edited cells per well [20]. Though these approaches help to enrich for the target mutation, the purified cells are the progeny of mixed colonies. Such inability to achieve homogeneity results in incomplete isogeneity, complicating subsequent phenotyping. Our single-cell cloning method mitigates these concerns and therefore offering a viable alternative for clonal isolation of iPSCs for gene editing studies.

Measuring editing efficiency. Addressing the aforementioned challenges through the combination of these independent techniques led to increased editing efficiency. To measure non-homologous end joining (NHEJ) editing frequency produced by our method, we

performed a T7 Endonuclease I (T7EN1) assay for the FACS-sorted positively transfected cell pool (> 5000 cells) of the three cell lines. We achieved editing efficiencies ranging between 48.6 to 57.5% for both the intronic and exonic regions of the *HPRT* and *FOXP2* genes across the iPSC lines; a rate among the highest reported in the literature [21,23] (Fig. 2b and Supplementary Table S2). We further confirmed these edits using Sanger sequencing of 20 single-cell clones from each cell line and observed comparable results to the transfected cell pool (Supplementary Fig. S2-S4). Relative to other methods, this approach has the advantage of fusing a crRNA and tracrRNA duplex to the Cas9 enzyme to form a single RNP capable of cleaving DNA almost immediately after delivery. This complex is subsequently degraded, meaning the RNP can only interacts with the genome for a relatively short period of time, thus decreasing the risk of re-cutting of the edited locus and increasing editing efficiency. This is the exact opposite to the long-term expression of Cas9 resulting from integration of the Cas9 enzyme into the genome through plasmid cloning [22,23]. It is of note that editing efficiency is locus and cell line dependant. As such, less successful editing may be observed within essential or loss-of-function intolerant genes, and may also be influenced by genetic background variability between cell lines [24].

Although the CRISPR-Cas9 complex can generate undesired off-target editing throughout the genome, this risk is reduced in our method with the use of non-integrative CRISPR delivery systems. The short half-life of RNPs within the cells further mitigates off-target cutting [25]. To measure this, we Sanger sequenced the top five off-target regions for all three cell lines of the FACS-sorted positively transfected cell pool (>5000 cells) along with their respective un-edited parental lines. Decomposition tracking of indels of the sequencing data using the Inference of CRISPR Edits (ICE) web tool (Synthego) showed no off-target editing in any untargeted loci (Supplementary Fig. S8 and Supplementary Table S3).

Assessment of genomic integrity and the pluripotent of the edited cells. To determine whether CRISPR-Cas9 genome editing led to complex chromosomal aberrations, we conducted karyotyping to examine the shape, size, and number of chromosomes in the edited cell lines relative to the parental lines. We observed the correct number of chromosomes with no aberrations in the three edited iPSC lines (Supplementary Fig S5-S7). In addition to maintaining genomic integrity, it is essential that the cell lines' pluripotency and differentiation potential is preserved post-CRISPR editing to ensure they retain their utility for disease modelling. Immunostaining for the pluripotency markers of OCT4, TRA-1-60, SOX2 and SSEA4 in the edited cell lines showed normal expression (Supplementary Fig S5-S7).

Furthermore, teratoma formation testing demonstrated that the edited cells could differentiate into all three germ layers, further confirming preservation of the pluripotent characteristics of these stem cells (Fig.3).

Conclusion

Collectively, our method addresses the key challenges posed by application of CRISPR-Cas9 DNA editing in human derived iPSCs by achieving (1) successful CRISPR-Cas9 transfection, (2) high rates of cell survival, (3) homogeneity/monoclonality, (4) reduced off-target effects, and (5) improved editing efficiency.

This easy and reliable method represents a quick and highly efficient approach that can be implemented with both non-homologous end-joining and SNP-based homology directed repair, as well as other CRISPR-based gene perturbation systems (e.g., CRISPR activation, and CRISPR interference). We anticipate that our approach will facilitate stem cell modelling of complex genetic conditions, bridging the gap between identification of genomic risk variants and their associated functional biology.

Methods

Guide RNA and primer design. The Alt-R CRISPR-Cas9 crRNA (CRISPR RNA) selection tool from Integrated DNA Technology (IDT) (https://sg.idtdna.com/site/order/designtool/index/CRISPR_PREDESIGN) was used to design the guide RNA (gRNA) targeting exon 2 of the Forkhead Box P2 (*FOXP2*) gene. Predesigned Alt-R CRISPR-Cas9 HPRT Positive Control crRNA (Integrated DNA Technologies, Cat#1079132) was also purchased to target intron 6-7 of the human Hypoxanthine Phosphoribosyltransferase 1 (*HPRT*) gene. Detailed sequences are provided in Supplementary Table S1. Primer sequences used to amplify the target regions and the top five potential off-target regions were designed using primer3plus (https://www. bioinformatics. nl/cgi-bin/primer3plus/primer3plus.cgi) [26] (see Supplementary Table S2-S3).

Pre-transfection iPSCs culture. Three human iPSC cell lines were used in this study: Peripheral blood mononuclear cells (PBMC)-derived MICCNi002-A [27], Human Dermal Fibroblasts, neonatal (HDFn) (Thermo Fisher Scientific, Cat#C0045C) and Human Dermal Fibroblasts, adult (HDFa) (Thermo Fisher Scientific, Cat#C0135C). All iPSC lines were seeded on Vitronectin (Thermo Fisher Scientific, Cat#A14700) coated plates and were maintained in Essential 8 Medium (Gibco, Cat#A1517001) supplemented with RevitaCell

(Gibco, Cat# A2644501) and 1X Penicillin-Streptomycin (Gibco, Cat#15140122) for the first 24 hours. Media were replaced every day with Essential 8 medium without RevitaCell until 60-80% confluency was achieved, allowing for up to three passages for cells to adapt and reach a healthy state with a minimum differentiation rate.

Construction of CRISPR transfection complex. The CRISPR-Cas9 system was purchased form IDT. One microliter of ALT-R CRISPR-CAS9 crRNA (100 µM) and Alt-R CRISPR-Cas9 tracrRNA (100 µM) conjugated with ATTO™ 550 (Cat#1075928) were added to 98 µL of Nuclease-free Duplex Buffer (Cat#11-01-03-01) to form the crRNA:tracrRNA duplex. The mixture was heated at 95°C for 5 minutes and allowed to cool for 30 minutes at room temperature. To assemble the ribonuclear protein (RNP) complex, 6 µL of an equimolar (1 µM) amount of diluted Cas9 Nuclease (Cat#1081058) and the RNA duplex were mixed with 13 µL of Opti-MEM Medium (Thermo Fisher Scientific, Cat#51985091). Following incubation for 5 minutes at room temperature, 2 µL of Lipofectamine Stem Transfection Reagent (Invitrogen, Cat#STEM00015) and 23 µL Opti-MEM medium were mixed and added to the 25 µL of RNP complex. The total CRISPR-Cas9 transfection complex (50 µL) was incubated for 20 minutes at room temperature.

iPSCs transfection with CRISPR complex. At 60-80% confluency, Versene solution (Gibco, Cat# 15040066) was added to the iPSC cell culture to gently detach growing cell clumps from the culture vessel surface and was subsequently aspirated following 5 minutes of incubation. Essential 8 medium supplemented with RevitaCell without antibiotic was added immediately to the cells, pipetting up and down several times to dissociate them into clusters of 3-10 cells. The cells were then counted and adjusted to 300,000 cell/ml. One hundred and fifty thousand cells were added to 50 µL of the total transfection complex pre-plated in a single well of a 24-well plate coated with Vitronectin. Following 24 hours, the media were changed to Essential 8 medium without RevitaCell and incubated for an additional 24 hours, after which they were ready for fluorescence-activated cell sorting (FACS).

Sorting the positively transfected cells. The cells were dissociated into single cells with Accutase (STEMCELL Technologies, Cat#07920) and centrifuged for 4 minutes at 200 x g. The cell palette was resuspended in 300 µL of FACS medium prepared with 4 mL of DMEM/F-12, HEPES, no phenol red (Gibco, Cat#11039021), 0.5 mL of CloneR supplement (STEMCELL Technologies, Cat#05889), 0.5 mL of E8 supplement (Gibco, Cat#A15171-01), 50 µL of (100X) Penicillin-Streptomycin (Gibco, Cat#15140122), 5 µL of DAPI (Cell

Signaling Technology, Cat#4083S), and 2 µL of 0.5 M EDTA (Invitrogen, Cat#15575020), and passed through a Falcon 5 mL tube with a cell strainer cap (Corning Cat#352235). This supplemented FACS medium enhances the survival of singularised iPSCs for the duration of sorting. Using a BD Influx Cell Sorter (BD Biosciences), the top 40% of ATTO-550 positive cells were sorted as single cells into individual wells of two 96-well plates coated with 10 µg/mL of CellAdhere Laminin-521 (STEMCELL Technologies, Cat#77004) containing StemFlex medium (Gibco, Cat#A3349401) supplemented with CloneR and incubated at 37°C for 48 hours. The remaining positive cells were bulk sorted in a single well of a Vitronectin coated 6-well plate containing Essential 8 medium and ROCK inhibitor (STEMCELL Technologies, Cat#72304) for the purpose of measuring editing efficiency of the experiment.

Post-FACS single-cell iPSC cell culture. Following 48 hours of incubation, a full CloneR-supplemented media change was performed. At day three, 25% of the initial seed volume of cloning media was added to each well. At day four, a full media replacement without CloneR supplement was performed and repeated every other day until the single-cell clones reached a confluency of ~60-80% for further analysis. On day 14, the total number of single-cell clones from each cell line were counted to obtain single-cell clone survival rate.

Measuring editing efficiency: T7E1 cleavage assay. Total genomic DNA from the FACS-sorted positively transfected cell pool (>5000 cells) of three biological replicates for HDFn, HDFa and MICCNi002-A were extracted using PureLink Genomic DNA Mini Kit (Invitrogen, Cat#K182001) and the *HPRT* and *FOXP2* target regions were amplified using PCRBIO HiFi Polymerase (PCR Biosystems, Cat#PB10.41-02) with primers listed in Supplementary Table S2.

The PCR products were digested with T7 endonuclease 1 enzyme using the Alt-R Genome Editing Detection Kit (Integrated DNA Technologies, Cat#1075931). The cleaved DNA fragments were run on an Agilent Fragment Analyzer system and analysed with the ProSize software (Agilent Technologies) to measure the size and quantify of the fragments to determine CRISPR gene editing efficiency. The frequency of the non-homologous end joining (NHEJ) was calculated using the Agilent Technologies formula:

$$\text{Percentage Editing Efficiency} = \frac{\textbf{Average Molarity (fragment 1 and fragment 2)}}{\textbf{Average Molarity (fragment 1 and fragment 2) + Molaity fragment uncut}}$$

To further confirm the achieved editing efficiency, 60 single-cell clones including 20 from each cell line were expanded in 6-well plate. DNA was extracted and amplified as described above.

The targeted PCR amplicons of *HPRT* and *FOXP2* from each clone were subsequently Sanger sequenced. The percentage of edited clones were calculated as the number of clones detected to possess at least one bp change relative to the total number of sequenced clones (Supplementary Fig. S2-S4).

Karyotyping. To discern whether the CRISPR-editing protocol induced chromosomal aberrations such as deletions, duplications, translocations, inversions, the edited single-cell clones from each cell line were externally Karyotyped and analysed using standard methods at Monash Health Pathology, Australia (Supplementary Fig. S5-S7).

Immunofluorescence. Pluripotency of the CRISPR-Cas9 edited single-cell clones was evaluated via immunostaining of OCT4, TRA-1-60, SOX2 and SSEA4 markers using the Pluripotent Stem Cell 4-Marker Immunocytochemistry Kit (Invitrogen, Cat#3A24881). The culturing media were aspirated, and the cells were incubated in fixative solution for 15 minutes, followed by 30 minutes of blocking, and incubating with the primary antibodies for 3 hours at 4°C. The cells were subsequently washed three times and further incubated with the appropriate secondary antibodies for 1 hour at room temperature. This was followed by further washing steps, with the last wash containing NucBlue Fixed Cell Stain (DAPI). The cells were immediately imaged with the EVOS M5000 Imaging System (Thermo Fisher Scientific, Cat# AMF5000) (Supplementary Fig. S5-S7).

Teratoma formation assay. Approximately 1 x 10^6 iPSCs from each of the three edited cell lines were injected into severe combined immunodeficiency disease (SCID) mice. Six weeks later, 1-2 cm diameter teratomas formed and were subsequently hematoxylin and eosin stained at the Monash Histology Platform to examine their ability to differentiate into each of endoderm, ectoderm, and the mesoderm germ layers (Fig. 3).

Measuring off-target effects. The top five off-target genomic regions of the transfected cell pool as well as the parental cell lines were amplified and Sanger sequenced. Results were compared to the wild type using the ICE; a Synthego web tool (https://www.synthego.com/products/ bioinformatics/crispr-analysis) which uses Sanger sequencing data to analyse the levels of insertions/deletions (indels) caused by CRISPR editing (Supplementary Table S3 and Supplementary Fig. S8) [28].

Statistical information. The samples for the T7EN1 assay and those for single-cell clone survival rate were all biological replicates (independent transfections). Reproducibility of the

transfection efficiency were tested across three different experiments. The single-cell clone survival and editing efficiencies were expressed as the mean of independent experiments ± SEM.

References

1 Gallagher, M. D. & Chen-Plotkin, A. S. The Post-GWAS Era: From Association to Function. *Am J Hum Genet* **102**, 717-730, doi:10.1016/j.ajhg.2018.04.002 (2018).

2 Hoffmann, A., Ziller, M. & Spengler, D. Focus on Causality in ESC/iPSC-Based Modeling of Psychiatric Disorders. *Cells* **9**, doi:10.3390/cells9020366 (2020).

3 Kampmann, M. CRISPR-based functional genomics for neurological disease. *Nat Rev Neurol* **16**, 465-480, doi:10.1038/s41582-020-0373-z (2020).

4 Matos, M. R., Ho, S. M., Schrode, N. & Brennand, K. J. Integration of CRISPR-engineering and hiPSC-based models of psychiatric genomics. *Mol Cell Neurosci* **107**, 103532, doi:10.1016/j.mcn.2020.103532 (2020).

5 Soldner, F. *et al.* Generation of isogenic pluripotent stem cells differing exclusively at two early onset Parkinson point mutations. *Cell* **146**, 318-331, doi:10.1016/j.cell.2011.06.019 (2011).

6 Gresch, O. *et al.* New non-viral method for gene transfer into primary cells. *Methods* **33**, 151-163, doi:10.1016/j.ymeth.2003.11.009 (2004).

7 Ihry, R. J. *et al.* p53 inhibits CRISPR-Cas9 engineering in human pluripotent stem cells. *Nat Med* **24**, 939-946, doi:10.1038/s41591-018-0050-6 (2018).

8 Das, D., Feuer, K., Wahbeh, M. & Avramopoulos, D. Modeling Psychiatric Disorder Biology with Stem Cells. *Curr Psychiatry Rep* **22**, 24, doi:10.1007/s11920-020-01148-1 (2020).

9 Zhang, X. H., Tee, L. Y., Wang, X. G., Huang, Q. S. & Yang, S. H. Off-target Effects in CRISPR/Cas9-mediated Genome Engineering. *Mol Ther Nucleic Acids* **4**, e264, doi:10.1038/mtna.2015.37 (2015).

10 Stewart, M. P., Langer, R. & Jensen, K. F. Intracellular Delivery by Membrane Disruption: Mechanisms, Strategies, and Concepts. *Chem Rev* **118**, 7409-7531, doi:10.1021/acs.chemrev.7b00678 (2018).

11 Ohgushi, M. *et al.* Molecular pathway and cell state responsible for dissociation-induced apoptosis in human pluripotent stem cells. *Cell Stem Cell* **7**, 225-239, doi:10.1016/j.stem.2010.06.018 (2010).

12 Chen, G., Hou, Z., Gulbranson, D. R. & Thomson, J. A. Actin-myosin contractility is responsible for the reduced viability of dissociated human embryonic stem cells. *Cell Stem Cell* **7**, 240-248, doi:10.1016/j.stem.2010.06.017 (2010).

13 Okamoto, S., Amaishi, Y., Maki, I., Enoki, T. & Mineno, J. Highly efficient genome editing for single-base substitutions using optimized ssODNs with Cas9-RNPs. *Sci Rep* **9**, 4811, doi:10.1038/s41598-019-41121-4 (2019).

14 Vakulskas, C. A. *et al.* A high-fidelity Cas9 mutant delivered as a ribonucleoprotein complex enables efficient gene editing in human hematopoietic stem and progenitor cells. *Nat Med* **24**, 1216-1224, doi:10.1038/s41591-018-0137-0 (2018).

15 Geng, B. C. *et al.* A simple, quick, and efficient CRISPR/Cas9 genome editing method for human induced pluripotent stem cells. *Acta Pharmacol Sin* **41**, 1427-1432, doi:10.1038/s41401-020-0452-0 (2020).

16 Singh, A. M. An Efficient Protocol for Single-Cell Cloning Human Pluripotent Stem Cells. *Front Cell Dev Biol* **7**, 11, doi:10.3389/fcell.2019.00011 (2019).

17 Yumlu, S. *et al.* Gene editing and clonal isolation of human induced pluripotent stem cells using CRISPR/Cas9. *Methods* **121-122**, 29-44, doi:10.1016/j.ymeth.2017.05.009 (2017).

18 Cobo, F. *et al.* Electron microscopy reveals the presence of viruses in mouse embryonic fibroblasts but neither in human embryonic fibroblasts nor in human mesenchymal cells used for hESC maintenance: toward an implementation of microbiological quality assurance program in stem cell banks. *Cloning Stem Cells* **10**, 65-74, doi:10.1089/clo.2007.0020 (2008).

19 Chen, Y. *et al.* Engineering Human Stem Cell Lines with Inducible Gene Knockout using CRISPR/Cas9. *Cell Stem Cell* **17**, 233-244, doi:10.1016/j.stem.2015.06.001 (2015).
20 Miyaoka, Y. *et al.* Isolation of single-base genome-edited human iPS cells without antibiotic selection. *Nat Methods* **11**, 291-293, doi:10.1038/nmeth.2840 (2014).
21 Wang, G. *et al.* Efficient, footprint-free human iPSC genome editing by consolidation of Cas9/CRISPR and piggyBac technologies. *Nat Protoc* **12**, 88-103, doi:10.1038/nprot.2016.152 (2017).
22 Zuris, J. A. *et al.* Cationic lipid-mediated delivery of proteins enables efficient protein-based genome editing in vitro and in vivo. *Nat Biotechnol* **33**, 73-80, doi:10.1038/nbt.3081 (2015).
23 Xu, X. *et al.* Efficient homology-directed gene editing by CRISPR/Cas9 in human stem and primary cells using tube electroporation. *Sci Rep* **8**, 11649, doi:10.1038/s41598-018-30227-w (2018).
24 Cahan, P. & Daley, G. Q. Origins and implications of pluripotent stem cell variability and heterogeneity. *Nat Rev Mol Cell Biol* **14**, 357-368, doi:10.1038/nrm3584 (2013).
25 Kim, S., Kim, D., Cho, S. W., Kim, J. & Kim, J. S. Highly efficient RNA-guided genome editing in human cells via delivery of purified Cas9 ribonucleoproteins. *Genome Res* **24**, 1012-1019, doi:10.1101/gr.171322.113 (2014).
26 Untergasser, A. *et al.* Primer3Plus, an enhanced web interface to Primer3. *Nucleic Acids Res* **35**, W71-74, doi:10.1093/nar/gkm306 (2007).
27 Tong, J. *et al.* Generation of four iPSC lines from peripheral blood mononuclear cells (PBMCs) of an attention deficit hyperactivity disorder (ADHD) individual and a healthy sibling in an Australia-Caucasian family. *Stem Cell Res* **34**, 101353, doi:10.1016/j.scr.2018.11.014 (2019).
28 Conant, D. *et al.* Inference of CRISPR Edits from Sanger Trace Data. *CRISPR J* **5**, 123-130, doi:10.1089/crispr.2021.0113 (2022).

Acknowledgements

This work has been supported by Project Grant funding from the National Health and Medical Research Council (NHMRC) of Australia to ZH (APP1146644).

Author contributions

A.N, X.L and Z.H designed the idea and planned the experiments. A.N performed all experiments except of teratoma formation assay which was performed by SM.L, G.S. Z.H, M.A.B, J.M.P and M.J.H developed the theory and conceived the study, contributed to the interpretation of the results, and oversaw the overall direction and planning. The manuscript was prepared by A.N, Z.H and K.P. All authors contributed to comments and editing.

Competing interests

The authors declare no competing interests.

Data availability

The Alt-R CRISPR-Cas9 crRNA (CRISPR RNA) selection tool is freely available at Integrated DNA Technology (IDT) (https://sg.idtdna.com/site/order/designtool/index/CRISPR_PREDESIGN). Primers designed using Primer3plus available at (https://www.bioinformatics.nl/cgi-bin/primer3plus/primer3plus.cgi). Decomposition tracking of indels in the off-target regions can be analysed using the Inference of CRISPR Edits (ICE) web tool available at (Synthego) (https://www.synthego.com/products/bioinformatics/crispr-analysis).

Ethics declaration

The teratoma assays for human stem cells and reprogrammed cells have been performed under the Monash University Animal Ethics Research number ERM # 26424.

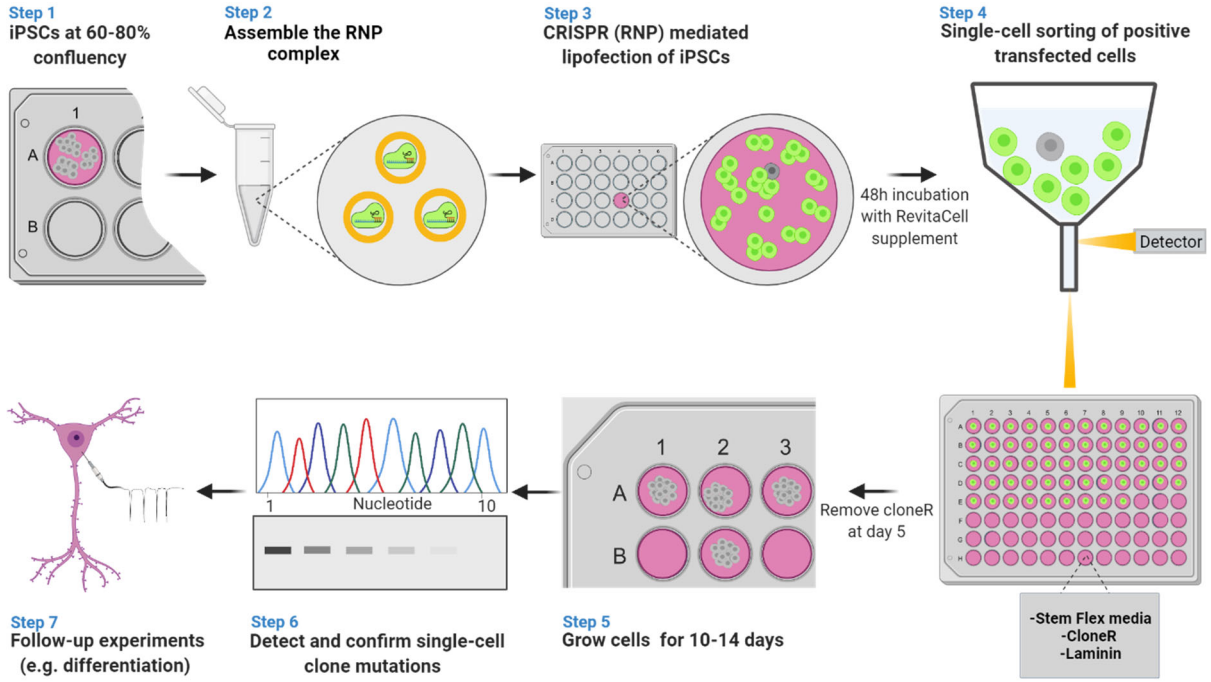

Figure 1. **Novel methodology for CRISPR-Cas9 editing of iPSCs**. **Step 1:** iPSCs are grown to 60-80% confluency. **Step 2:** The ribonucleoprotein complex (RNP) consisting of crRNA: tracrRNA duplex and Cas9 protein is formed and transfected within the small clusters of iPSC cells using Lipofectamine Stem Transfection Reagent **(Step 3)**. **Step 4:** Following 48 hours of incubation, positively transfected cells are single-cell sorted in a rich environment containing StemFlex medium and CloneR supplement in wells coated with Laminin. **Step 5:** Single-cells are grown for 10-14 days until they form a homogeneous single-cell clone and reach sufficient confluency for expansion. **Step 6:** A portion of the clones are selected for detection and confirmation of the desired mutations (e.g., Sanger sequencing, western blotting) and the remainder utilised for follow-up phenotyping experiments **(Step 7)**. Figure created with BioRender.com.

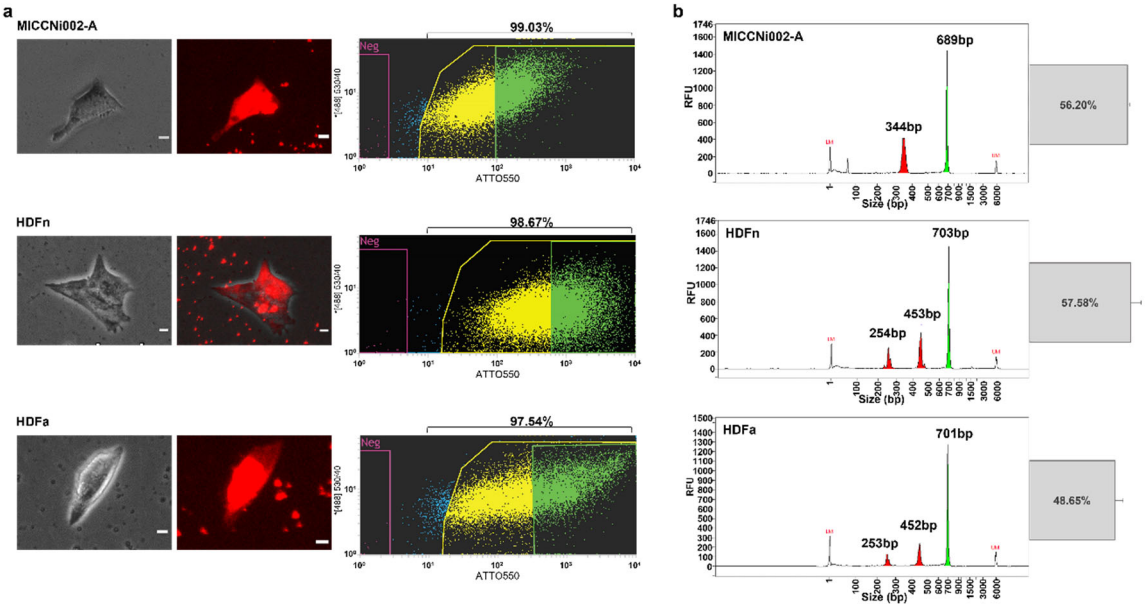

Figure 2. Our methodology shows high transfection and editing efficiency while achieving homogeneity and a high-rate single-cell clone survival. (a) Three different iPS cell lines (MICCNi002-A, HDFn and HDFa) were transfected with the ribonucleoprotein complex, and the transfection efficiencies were measured with fluorescence microscopy and flowcytometry after 48 hours. From left to right are the cell bright field images, fluorescence images, and flowcytometry dot plot. The flowcytometry dot plot shows >97% transfection efficiency (yellow and green) Scale bar,10 µm. **(b)** Electropherograms of T7EN1 digested pool samples run on a fragment analyser for each of the three edited iPSC lines showing the full length (green) and cleaved fragments (red). The CRISPR-Cas9 editing method achieved an editing in the range of 48.6 to 57.5% in the targeted loci of the three cell lines. The peaks are colour-coded for easy identification. RFU: Relative Fluorescence Unit LM: lower marker, UM: upper marker.

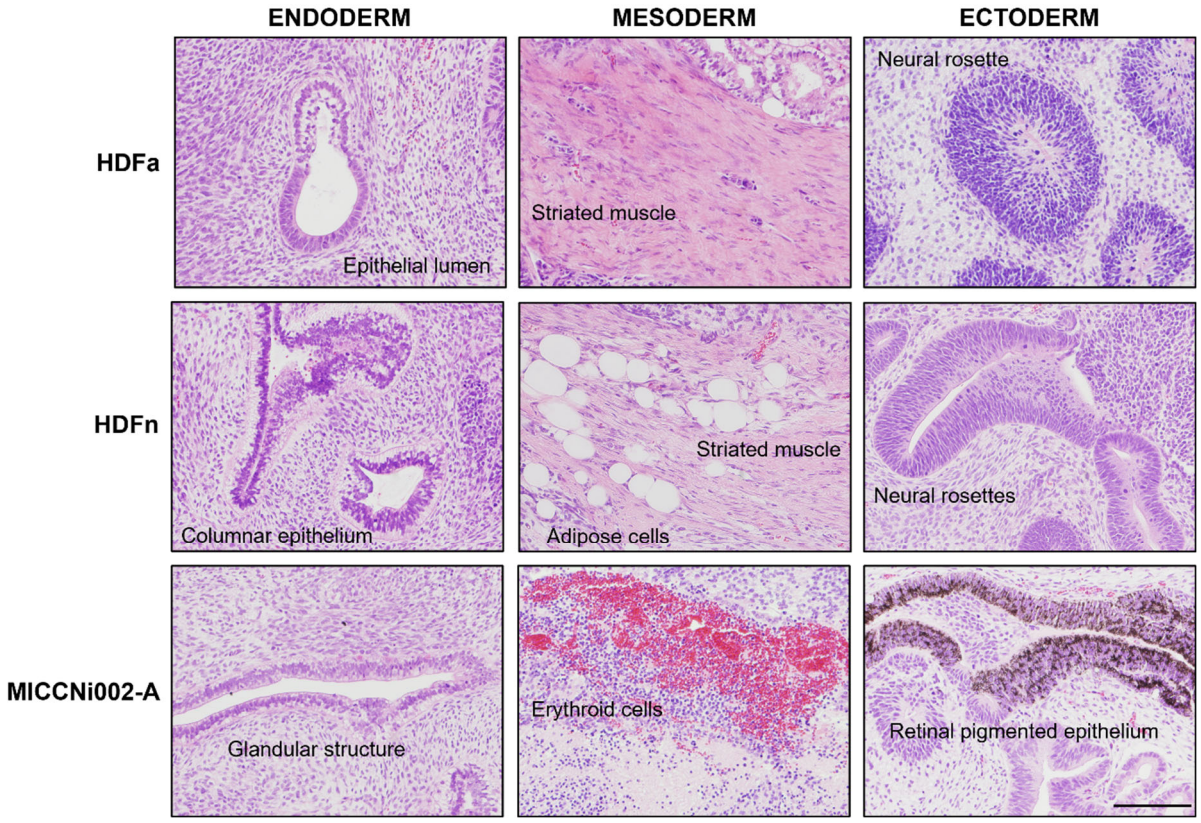

Figure 3. **Assessment of differentiation potential of edited iPSC using teratoma formation assay.** Histopathological assessment of the three edited iPSC lines is labelled on the left-hand side. Brightfield micrographs of hematoxylin and eosin-stained histological sections show cells that contain derivatives of the 3 germ layers: endoderm (first column), mesoderm (second column) and ectoderm (third column). The endodermal tissues of the teratomas include epithelial, columnar epithelium, and glandular structure. The mesodermal tissues of the teratomas include striated muscle, adipose cells, and erythroid cells. The ectodermal tissues of the teratomas include neural rosette structures and retinal pigmented epithelium. Scale bar: 200 μm.